PHYSICS AND CHEMISTRY OF SOLID STATE
V. 24, No. 1 (2023) pp. 106-113
Section: Physics

DOI: 10.15330/pcss.24.1.106-113

Vasyl Stefanyk Precarpathian National University

ФІЗИКА І ХІМІЯ ТВЕРДОГО ТІЛА
Т. 24, № 1 (2023) С. 106-113
Фізико-математичні науки

PACS:75.50.Tt ISSN 1729-4428

Yu. Nykyruy[1], S. Mudry[1], Yu. Kulyk[1], V. Prunitsa[1], A. Borysiuk[2]

Magnetic properties and nanocrystallization behavior of Co-based amorphous alloy

[1]*Metal Physics Department, Ivan Franko National University of Lviv, Lviv, Ukraine,yuliya.nykyruy@lnu.edu.ua*
[2] *Department of Applied Physics and Nanomaterial Science, Lviv Polytechnic National University, Lviv, Ukraine*

The magnetic properties of the amorphous $Co_{57}Fe_5Ni_{10}Si_{11}B_{17}$ alloy have been studied by a vibrating sample magnetometer. The temperature dependence of saturation magnetization was measured and the Curie point and crystallization onset temperature were determined as 560 K and 760 K respectively. The coercive force was obtained as 200 A/m and saturation magnetization - 65 Am^2 /kg. The alloy was produced in the form of a ribbon thickness of 30 μm using the melt spinning method, and its internal amorphous structure was examined by the X-ray diffraction method. The crystallization behavior of the alloy was studied using series of isothermal annealing of the samples of the alloy at temperatures in the range of 723-1023 K for different exposures (up to 240 minutes) and nanocrystalline phases were detected by the X-ray diffraction analysis.

Keywords: Co-based amorphous alloy, DTA, thermo-magnetic curves, hysteresis, magnetic properties, X-ray diffraction, nanocrystallization.

Received 01 November2022; Accepted 21 February2023.

Introduction

Co-based amorphous alloys are attractive materials that are already used in various fields of industry. They are very soft magnetic, provide a sufficient high saturation magnetization and are zero-magnetostrictive for appropriate chosen concentration of alloy. Co-based amorphous ribbons are attractive alternative as detection layer in magnetoresistive systems [1]. Depending on the type of hysteresis loop these materials are used in current and power transformers, sensor elements, choke coils, magnetic screens/shielding, high-frequency power applications, etc [2, 3, 4]. Rapidly quenched Co-based alloys were proposed as suitable materials for magnetic cores working at high frequencies. Compositions with zero magnetostriction, magnetic properties and crystallization onset temperatures T_x in $(Fe_aCo_{1-a-b}Ni_b)_{100-y}(Si_{0,4}B_{0,6})_y$ system as function of Ni (Mo, Mn) and metalloid content were investigated in [5]. The main disadvantage of these amorphous metal alloys (AMA) was the fact that Curie point exceeds crystallization onset temperature that complicates an effective heat treatment on hysteresis loop shape. In previous our research the amorphous alloys with similar chemical composition Co-(FeMoMn)-(SiB) were investigated and slightly different thermal stability and magnetic properties were revealed [6]. The Curie point of these alloys doesn't exceed crystallization onset temperature, allowing carrying out the optimization annealing. So, a slight variation in the percentage of elements significantly changes the thermal stability and Curie point of these alloys and Ni doping/absence effect on properties. In this paper, we present the results on studies of magnetic properties and crystallization behavior of $Co_{57}Fe_5Ni_{10}Si_{11}B_{17}$ amorphous alloy in comparison with other composition of the system

I. Materials and methods

The amorphous alloy $Co_{57}Fe_5Ni_{10}Si_{11}B_{17}$ was produced by rapid cooling from the melt using the melt-spinning technique in the form of the ribbon. The ribbon thickness is about 25 μm and width about 1.5 cm respectively.

Magnetic measurements were performed using a vibrating sample magnetometer. Re-magnetization curves of the studied samples were recorded in a magnetic field from –300 kA/m to +300 kA/m. Since the use of saturating magnetic fields is a prerequisite for performing quantitative magnetic phase analysis, the specific saturation magnetization (σ_s) and its temperature dependence were measured in the magnetic field of 800 kA/m. Heating was performed at the rate of 5 K/min within the temperature range of 293 - 950 K.

The as-obtained ribbons were investigated by the DTA-method using synchronous thermal analyzer Linseis STA PT 1600 under dynamic argon atmosphere (~6 liters per hour). Heating was performed at the rate of 10 K/min from 293 K up to 973 K.

To study the structural and phase transformations induced by heat treatment, a series of isothermal annealing of samples of the amorphous alloy $Co_{57}Ni_{10}Fe_5Si_{11}B_{17}$ were carried out. Annealing was performed in an air atmosphere at temperatures T=723°K, 773°K, and 823°K with different exposure times of up to 240 minutes. The diffraction curves of the annealed samples were measured on a DRON-3 automated X-ray diffractometer using Cu-K_α radiation, monochromatized by reflection from a pyrolytic graphite single crystal mounted on a diffracted beam, which makes it possible to completely to avoid the sample's fluorescent radiation. The back-scattered diffraction curves of the samples were recorded in the mode of continuous movement of the detector at a speed of 2 degrees per minutes with automatic registration of the intensity of scattered radiation.

II. Results and discussions

Re-magnetization curves of the magnetic moment for the $Co_{57}Ni_{10}Fe_5Si_{11}B_{17}$are presented in Fig.1a and show that in the region of weak magnetic fields the magnetization increases in proportion to the external strength magnetic field, and in a strong magnetic field (above 17-20 kA/m) the saturation is observed. The specific saturation magnetization was obtained as σ_s=65A*m^2/kg. The saturation requires quite a strong magnetic field, while the residual magnetization is small. The coercive force H_C was obtained as about 200 A/m, which corresponds to the average values of coercive force for soft magnetic materials [7], but it is quite larger than the values H_C for some Co-Si-B-based alloys obtained in [8, 9, 10, 11]. Worth noting, the coercive force is structurally sensitive and depends on elastic stresses, shape, and dimension of the ferromagnetic phases. The magnetization of the amorphous ribbon occurs by slightly shifting the boundaries of the domains and the reverse rotation of the vector of spontaneous magnetization.

The temperature dependence of specific saturation magnetization (thermomagnetic curves) $\sigma_s(T)$ for the as-quenched Co-based amorphous alloy (Fig.1b) is typical for amorphous ferromagnets. The saturation magnetization decreased with temperature increasing to Curie point (T_C = 560 K). The Curie point of the amorphous alloy was determined by constructing a model of temperature dependence of the spontaneous saturation magnetization of the alloy according to the Weiss–Heisenberg theory. The Curie temperature marks the ferromagnetic - paramagnetic transition, at which $\sigma_s \rightarrow 0$. The temperature interval of ferromagnetic phase existence for $Co_{57}Fe_5Ni_{10}Si_{11}B_{17}$ is wary wide, about ~200 K. Further increase of temperature resulted in σ_s increasing caused by the crystallization of ferromagnetic phase with higher Curie temperature. Thus, the temperature of σ_s increasing indicates the onset of amorphous-crystalline transition and means the crystallization onset temperature of this alloy as T_x=760K, determining the temperature limit of the amorphous state stability. At temperatures above T_x, the thermomagnetic curve displays the crystallization processes of the alloys. In the temperature range 760–950 K the curve is characterized by two intervals of increasing that could be interpreted as the formation of two crystallization phases and the crystallization process of the alloy proceeds through a multi-stage model [12]. The crystallization onset temperature of the second phase is determined as about 826 K. Saturation magnetization σ_s, coercive force H_C, Curie temperature T_C, and crystallization onset temperature $T_x$of the $Co_{57}Fe_5Ni_{10}Si_{11}B_{17}$ alloy are summarized in Table 1.

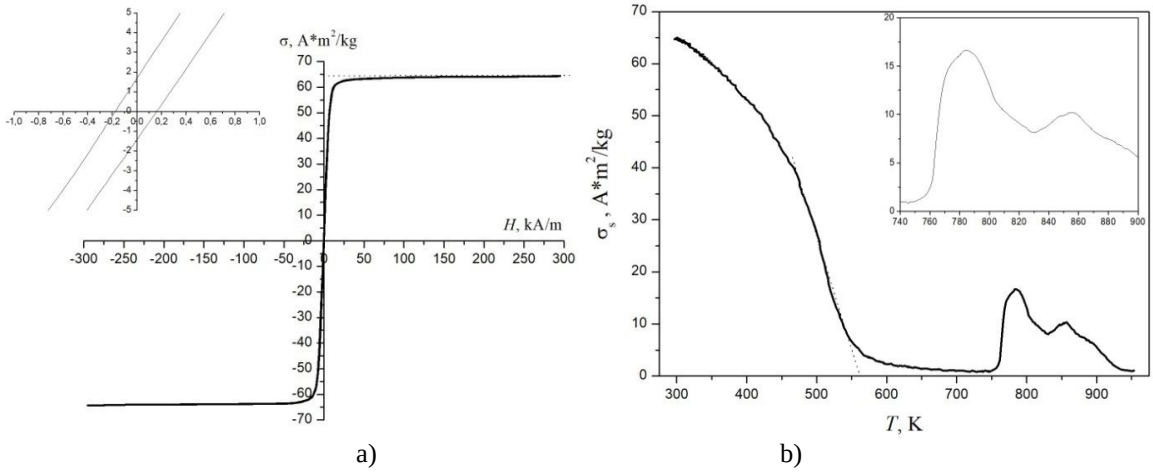

a) b)

Fig. 1. The hysteresis (a) and thermo-magnetic (b) curves of the $Co_{57}Fe_5Ni_{10}Si_{11}B_{17}$ alloy.

Table 1.

Results of magnetic measurements

Alloy composition	σ_s, Am^2 /kg	H_c, A/m	T_C, K	T_x^{TM}, K
$Co_{57}Ni_{10}Fe_5Si_{11}B_{17}$	65	200	560	760 826

The DTA curve for the as-quenched amorphous ribbon (Fig.2) is characterized by two endothermic peaks at a temperature above 780 K that correlates with thermomagnetic curve. The presence of two exothermic peaks has been interpreted as the formation of a second crystallization phase, and the crystallization process of the alloy proceeds through a two-stage model. The onset point of the first peaks specifies the crystallization onset temperature of the alloys indicating the start of the nanocrystallization process as well as the temperature limit of amorphous phase stability. For Co-Fe-Ni-Si-B alloys, the temperature range of amorphous phase stability is in the range of about 750-850 K and depends on impurities and the production process [13, 14, 15].

The results of thermomagnetic measurements are consistent with the DTA results; however, the value of T_x obtained by the DTA method is higher than T_x obtained by thermomagnetic curve. This difference can be explained partially by different heating rates at DTA and thermomagnetic measurements, because increasing the heating rate contributes to the shift of maxima to higher temperatures [16, 17].

To study the structure and phase transformations in the process of heat treatment, a series of isothermal annealing samples of the amorphous alloy were carried out. Fig. 3 shows the scattering intensity curves of samples annealed at T=723°K in the time interval from 5 to 240 min. The initial sample is characterized by a completely amorphous structure, which is indicated by the presence of broad maxima without intensity peaks from the

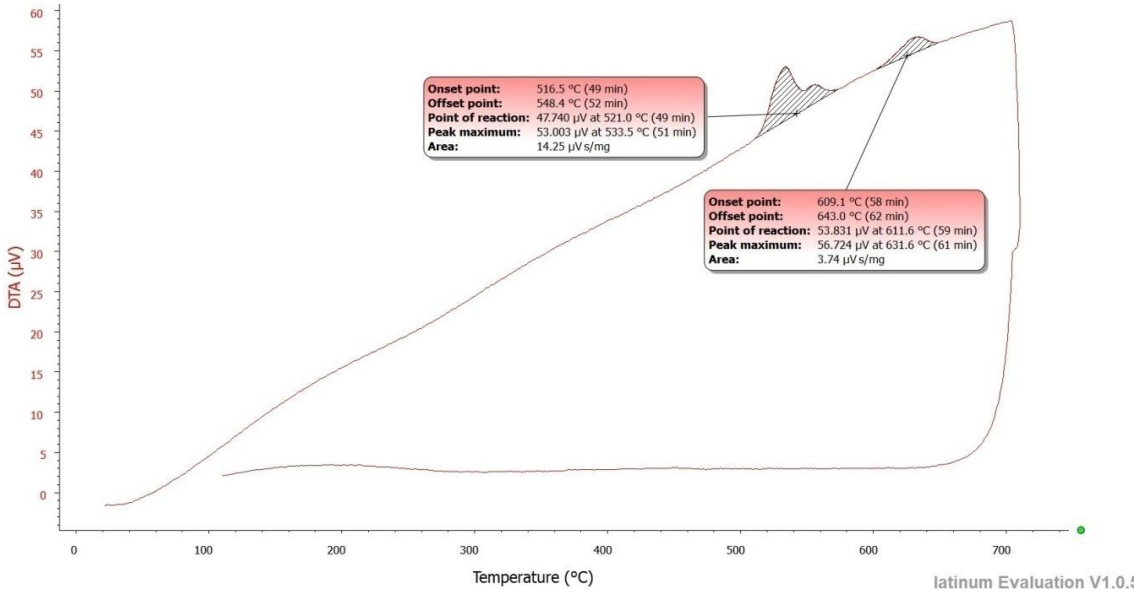

Fig. 2. The DTA curve of the $Co_{57}Fe_5Ni_{10}Si_{11}B_{17}$ alloy.

Table 2.

Results of DTA measurements

Alloy	Peak	Onset point, K	Offset point, K	Point of reaction, K	Peak maximum, K	Area µVs/mg
$Co_{57}Fe_5$ $Ni_{10}Si_{11}B_{17}$	1	789,65	821,55	794,15	806,65	14.25
	2	882,25	916,15	884,75	904,75	3.74

Table 3.

Characteristic temperature of phase transformations of the Co-(FeMoMnNi)-(SiB) alloys

Alloy No.	Chemical composition	T_{x1} K (by TM)	T_{x2} K (by TM)	T_{x1} K (by DTA)	T_{x2} K (by DTA)	T_C K	Ref.
1	$Co_{57}Fe_5$ $Ni_{10}Si_{11}B_{17}$	760	826	790	880	560	This article
2	$Co_{70}Fe_3Mo_{1.5}Mn_{3.5}Si_{11}B_{11}$	749	-	789	-	649	[6]
3	$Co_{73}Fe_1Mo_1Mn_3Si_{13}B_9$	704	798	729	824	683	[6]
4	$Co_{73.2}Fe_{4.3}Mn_{0.5}Si_{5.3}B_{16.7}$	718		710	813	731	[5]
5	$Co_{73}(Fe,Ni,Mo,Mn)_{5,7}(Si_{0,2}B_{0,})_{21,3}$	696		700	835	718	[5]
6	$Co_{73,3}(Fe,Ni,Mo,Mn)_{5,7}(Si_{0,2}B_{0,8})_{21}$	698		690	832	720	[5]
7	$Co_{58,3}(Fe,Ni,Mn)_{21,6}(Si_{0,2}B_{0,8})_{20,1}$	638		670	801	690	[5]
8	$Co_{55,7}(Fe,Ni,Mn)_{24,2}(Si_{0,2}B_{0,8})_{20,1}$	671		671	799	690	[5]

crystalline phase in the diffraction curve.

The position of the main maximum corresponds to the modulus of the wave vector s_1 = 31.3 nm^{-1}. The average interatomic distance is calculated by the Ehrenfest formula: $R_1 = \frac{7.73}{s_1}$, and is about 0.247 nm which is close to the sum of the atomic radii of Co equal to 0.250 nm. The size of the regions of coherent scattering, estimated according to the formula $L = \frac{2\pi}{\Delta s_1}$, where Δs_1 – the main maximum's full width of half-peak (FWHP), does not exceed 1.5 nm. This value is close to the results obtained for similar alloy composition in [18, 19] where the size of the regions of coherent scattering was 1.3-1.7 nm

Increasing the duration of the isothermal annealing leads to certain structure and phase transformations, which are especially pronounced in the sample annealed for 240 min (Fig. 1a). Against the background of the main maximum of the amorphous phase, a number of features appeared at the positions of s=29.1 nm^{-1}, 31.2nm^{-1}, and 32.8 nm^{-1}, which correspond to the diffraction lines (100), (002), and (101) of the α(Co) phase (hexagonal syngony, space group P63/mmc). The obtained result indicates the separation of the nanocrystalline phase of a solid solution based on α(Co) from the amorphous phase. For a more detailed analysis of structure and phase transformations, the difference curves of the scattering intensity were calculated by the formula: $I_d(s) = I(s) - I_0(s)$, where $I_0(s)$ - scattering intensity of the original amorphous alloy (Fig 1b).

As can be seen from Fig. 1b, some structure ~~structure~~ changes have begun to appear already during annealing within 15 minutes. Worth noting, the scattering intensity has increased in the region of the main maximum in the samples annealed for 15-30 minutes. The obtained result can be explained by the formation of nanocluster structure units with short-range order characteristic of hexagonal modification of the α(Co) in the amorphous phase. The size of the coherent scattering regions of α(Co) nanoclusters, estimated by FWHP of the maximum of the difference curves, reached L≈3.5 nm, which is significantly larger compared to the original amorphous phase (L≈1.5 nm). Regarding the samples annealed for a longer period of time (60-240 min.), a number of features corresponding to the (100), (002), and (101) lines of α(Co) have appeared on the difference curves. Thus, it can be assumed that an increasing of the duration of isothermal exposure causes the transformation of nanocluster structural units into α(Co) nanocrystals, the average size of which reached about 10 nm when the exposure time increased to 240 min. The volume fraction of the nanocrystalline phase does not exceed 20% of the volume of the amorphous alloy. The formation of α(Co) nanocrystals in the amorphous phase corresponds to the 1st peak on the DTA curve.

Let's consider changes in the structure-phase state of the $Co_{57}Ni_{10}Fe_5Si_{11}B_{17}$ amorphous alloy when the exposure temperature increased. As can be seen from Fig. 4, annealing of the samples for 5 min. at T=773ºK has not lead to a change in the phase state of the sample. However, it should be noted that the size of the coherent scattering

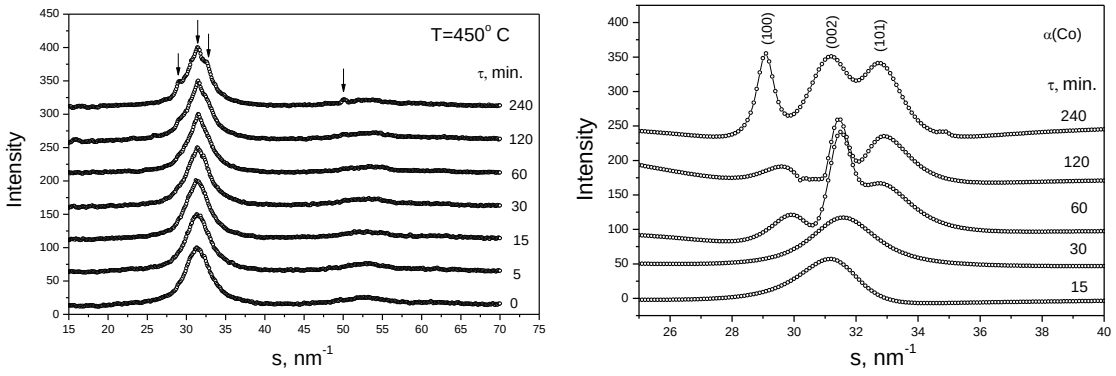

a) b)

Fig. 3. Diffraction curves of amorphous $Co_{57}Ni_{10}Fe_5Si_{11}B_{17}$ alloy annealed at T=723ºK (a), difference curves of scattering intensity (b).

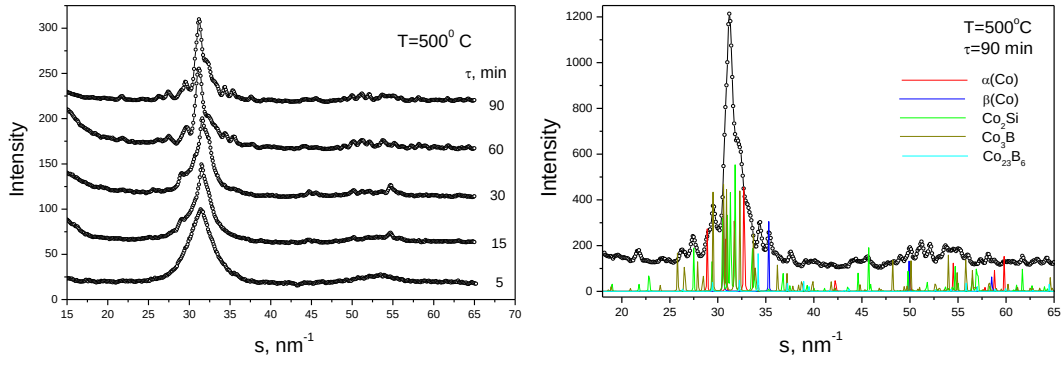

a) b)

Fig. 4. Diffraction curves of amorphous $Co_{57}Ni_{10}Fe_5Si_{11}B_{17}$ alloy annealed at T=773ºK (a), and curve decryption for T=773°K for 90 minutes (b).

regions of the amorphous phase has increased to 2.0 nm, which can be explained by the formation of nanocluster structural units with a short-range order of the α(Co) phase. Phase transformations in the sample started when the duration of annealing increased to 15 min. As can be seen from the diffraction patterns (Fig. 4a), in the time interval of 15-30 minutes the nanocrystals (of the hexagonal phase of an α(Co) based solid solution) are separated from the amorphous phase. Increasing the time of isothermal exposure to 60-90 minutes leads to the complete disintegration of the amorphous phase.

The diffraction spectrum of the sample annealed at *T*=773°K for 90 minutes, compared with the diffraction spectra of the phase components formed as a result of the decomposition of the amorphous phase, is shown in Fig. 4b. It can be represented as a superposition of the spectra of phases α(Co) (hexagonal syngony, group P63/mmc), β(Co) (cubic syngony, group Fm3m), silicide Co_2Si (orthorhombic syngony, group Pnma), boride Co_3B (orthorhombic syngonia, group Pnma), and boride $Co_{23}B_6$ (cubic syngonia, group Fm3m).

The parameters of the crystal structure of the phases are given in the Table. 4. As can be seen from the DTA data, the 1st maximum has a bifurcated form and can be

Table 4.

Parameters of the structure-phase state of the annealed amorphous alloy $Co_{57}Ni_{10}Fe_5Si_{11}B_{17}$

Temperature, annealing time	Phase composition	Unit cell parameters, Å	Average crystallite size, nm
773°K, 30 min.	α(Co)	a=2.5184±0.0007 c=4.0706±0.0015	22.0
	Co_2Si	a=4.9146±0.0012 b=3.7402±0.0011 c=7.1344±0.0021	21.5
	Co_3B	a=5.2349±0.0012 b=6.7101±0.0018 c=4.4239±0.0009	24.5
773°K, 90 min.	α(Co)	a=2.5044±0.0007, c=4.0193±0.0013	14.5
	β(Co)	a=3.5484±0.0008	75.0
	Co_2Si	a=4.8924±0.0010 b=3.7684±0.0009 c=7.1434±0.0016	25.5
	Co_3B	a=5.2015±0.0010 b=6.7211±0.001 c=4.4151±0.0008	19.0
	$Co_{23}B_6$	a=10.8216±0.0018	31.0
823°K, 5 min.	α(Co)	a=2.5172±0.0008, c=4.0746±0.0025	17.5
	Co_2Si	a=4.9212±0.0009 b=3.7705±0.0012 c=7.1066±0.0019	27.0
	Co_3B	a=5.2114±0.0013 b=6.7322±0.0016 c=4.4500±0.0009	26.0
823°K, 60 min.	α(Co)	a=2.5507±0.0003, c=4.0708±0.0005	125.0
	β(Co)	a=3.5473±0.0005	60.0
	Co_2Si	a=4.8999±0.0006 b=3.7450±0.0005 c=7.1236±0.0010	25.0
	Co_3B	a=5.2071±0.0008 b=6.6564±0.0011 c=4.3863±0.0007	50.0
	$Co_{23}B_6$	a=10.7446±0.0011	22.0
1023°K, 60 min.	α(Co)	a=2.4977±0.0003, c=4.0868±0.0011	24.0
	β(Co)	a=3.5273±0.0005	35.5
	Co_2Si	a=4.9271±0.0005 b=3.7596±0.0004 c=7.1468±0.0008	28.0
	Co_3B	a=5.2735±0.0006 b=6.6805±0.0008 c=4.3949±0.0006	34.0

considered as a superposition of two submaxima with different magnitudes of the thermal effect. If the 1st sub-maximum can be associated with the separation of α(Co) solid solution crystals, then the 2nd sub-maximum probably corresponds to the complete decomposition of the amorphous phase.

Let's consider the sequence of structural and phase changes in samples of the amorphous alloy $Co_{57}Ni_{10}Fe_5Si_{11}B_{17}$ when the isothermal exposure temperature increases to T=823°K. As can be seen from the series of diffraction patterns (Fig. 5a), crystallization processes occurred already at the early stages of isothermal annealing. Analysis of the phase composition of samples annealed for 2-5 minutes revealed the presence of highly dispersed phases: a solid solution based on α(Co), silicide Co_2Si, and borides Co_3B and $Co_{23}B_6$. Complete disintegration of the amorphous phase was observed when the duration of annealing was increased to 15 min. Fig. 5b shows the diffraction pattern of the sample annealed at 823°K for 60 minutes in comparison with reference diffraction spectra of phase components. It should be noted that the sample contains the same phases that we observed in the sample annealed at 773°K for 90 minutes.

Of great interest is the nature of phase transformations of amorphous Co-based alloys in the high-temperature region. Fig. 6 shows the diffraction pattern of a sample of the $Co_{57}Ni_{10}Fe_5Si_{11}B_{17}$ amorphous alloy annealed at T=1023°K for 60 minutes. As can be seen, the diffraction pattern of the sample can be represented as a superposition of diffraction spectra of phases based on α(Co), β(Co), Co_2Si, and Co_3B. It should be noted a significant increase in the proportion of cubic β(Co) modification, which is caused by the polymorphic transformation α(Co)→β(Co) (2nd maximum on the DTA thermogram). In addition, there are no phase lines of the metastable boride $Co_{23}B_6$ in the diffraction pattern, which indicates its decay and transformation into a stable modification of Co_3B according to the scheme $Co_{23}B_6 \rightarrow Co_3B + \beta(Co)$.

It is known some amorphous-nanocrystalline alloys have physical properties that ~~that~~ are better than the properties of both amorphous and nanocrystalline materials. For example, their magnetic properties are better than the magnetic properties of amorphous ferromagnetic alloys and they have high strength, much higher than the strength of amorphous or crystalline states [20]. The grain size of the nanocrystalline structure of the alloy is determined by the crystallization mechanisms associated with the chemical composition and thermodynamic characteristicse. An amorphous-nanocrystalline structure is often achieved by optimization annealing. The crystallization behaviours studies carried out in this work can be used to select optimization annealing modes, which is the aim of our further research.

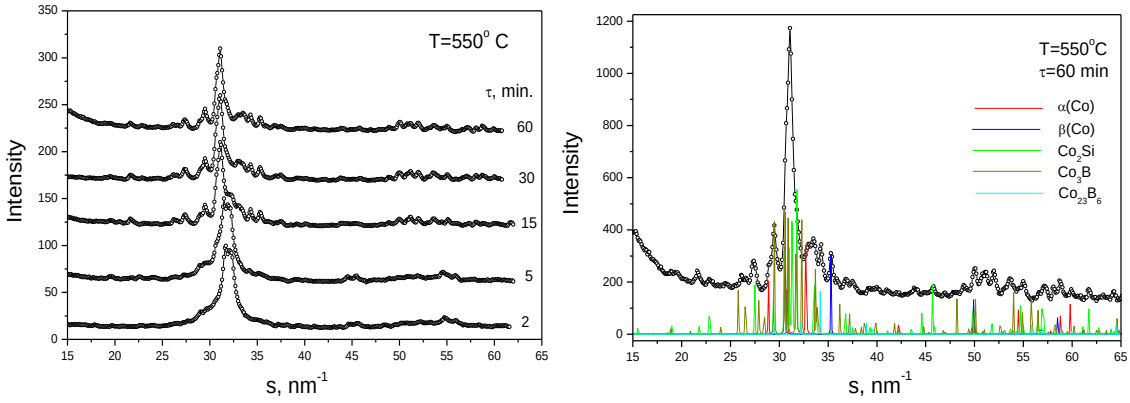

Fig. 5. Diffraction curves of amorphous $Co_{57}Ni_{10}Fe_5Si_{11}B_{17}$ alloy annealed at T=823°K (a), and at T=823°K for 60 minutes (b).

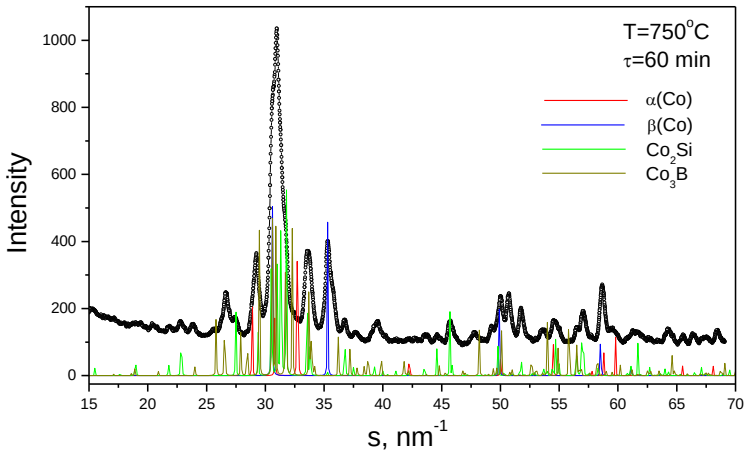

Fig. 6. Diffraction pattern of the sample annealed at T=1023°K for 60 minutes.

Conclusions

Magnetic properties and crystallization behavior of the $Co_{57}Ni_{10}Fe_5Si_{11}B_{17}$ amorphous alloy produced by the melt-spinning technique were studied and parameters that can be useful for practical applications were observed. Our results show that the Curie point of the investigated material is much smaller than the crystallization onset temperature, allowing optimization annealing. The temperature of optimization annealing should not significantly exceed 723 K at the exposure time of 1-4 hours due to the formation of borides.

Funding

This research did not receive any specific grant

Declaration of competing interest

The authors declare that they have no known competing financial interests or personal relationships that could have appeared to influence the work reported in this paper.

Nykyruy Yu. – PhD, Associate Prof. of Metals physics department;
Mudry S.– Prof., D.Sc. Head of Metal physics department;
Kulyk Yu. – PhD, Senior engineer of Metal physics department;
Prunitsa V.– PhD student of Metal physics department
Borysiuk A. – Senior researcher of Department of Applied Physics and Nanomaterial Science.

[1] A. Kaufler, Y. Luo, K. Samwer, G. Gieres, M. Vieth, J. Wecker, *Tunnel-magnetoresistance system with an amorphous detection layer*, Journ. Appl. Phys. 91, 1701 (2002); https://doi.org/10.1063/1.1426236.
[2] R. Hasegawa, *Applications of amorphous magnetic alloys*, Mater. Sci. Eng., A 375–377,90 (2004); https://doi.org/10.1016/j.msea.2003.10.258.
[3] K. Ackland, A. Masood, S. Kulkarni, P. Stamenov, *Ultra-soft magnetic Co-Fe-B-SiNb amorphous alloys for high frequency power applications*, AIP Adv., 8, 56129(2018);https://doi.org/10.1063/1.5007707.
[4] A.V. Nosenko, V.V. Kyrylchuk, M.P. Semen'ko, M. Nowicki, A. Marusenkov, T. M. Mika, et al., *Soft magnetic cobalt based amorphous alloys with low saturation induction*, J. Magn. Magn Mater. 515, 167328 (2020);https://doi.org/10.1016/j. jmmm.2020.167328.
[5] V K Nosenko, V V Maslov, A P Kochkubey and V V Kirilchuk, *New soft magnetic amorphous cobalt based alloys with high hysteresis loop linearity*, J. Phys.: Conf. Ser. 98, 072006 (2008);https://doi.org/10.1088/1742-6596/98/7/072006.
[6] Y. Nykyruy , S. Mudry , Y. Kulyk , A. Borisyuk,Magnetic properties and nanocrystallization process in Co-(Me)-Si-B amorphous ribbons, Applied Nanoscience, (2022); https://doi.org/10.1007/s13204-022-02746-6.
[7] Konieczny, Jaroslaw & A, Borisjuk & M, Pashechko & Dobrzanski, Leszek, *Magnetic properties of Co-based amorphous ribbon under cyclic heating and cooling*, Journal of Achievements in Materials and Manufacturing Engineering, 42 (1-2), 42 (2010);
[8] Anton V. Nosenko, Vasyl V. Kyrylchuk, Mykhailo P. Semen'ko, Michał Nowicki, Andriy Marusenkov, Taras M. Mika, Oleksandr M. Semyrga, Galyna M. Zelinska, Viktor K. Nosenko, Soft magnetic cobalt based amorphous alloys with low saturation induction, Journal of Magnetism and Magnetic Materials, Volume 515, 2020, 167328, ISSN 0304-8853; https://doi.org/10.1016/j.jmmm.2020.167328.
[9] V K Nosenko et al., *New soft magnetic amorphous cobalt based alloys with high hysteresis loop linearity*, J. Phys.: Conf. Ser., 98, 072006 (2008);https://doi.org/10.1088/1742-6596/98/7/072006.
[10] S. Lesz, R. Babilas, M. Nabiałek, M. Szota, M. Dośpiał, R. Nowosielski, *The characterization of structure, thermal stability and magnetic properties of Fe–Co–B–Si–Nb bulk amorphous and nanocrystalline alloys*, Journal of Alloys and Compounds, 509, Supplement 1, S197 (2011);https://doi.org/10.1016/j.jallcom.2010.12.146.
[11] V. V.Girzhon, A. V. Smolyakov, N. I.Zakharenko, N. G.Babich, &M. P.Semen'ko, *Effect of pulsed laser heating on the magnetic properties of amorphous alloy 30KSR*, The Physics of Metals and Metallography, 111(6), 561 (2011); https://doi.org/10.1134/s0031918x11050061.
[12] A.K. Panda, S. Kumari, I. Chattora, P. Svec, A. Mitra, Effect of Fe addition on the crystallization behaviour and Curie temperature of CoCrSiB-based amorphous alloys, Philos. Mag. 85 (17), 1835 (2005);https://doi.org/10.1080/14786430500098934.
[13] N. I. Noskova, *Structure and Magnetic Properties of Iron- and Cobalt-Based Amorphous Alloys Versus Nanocrystallization Conditions*. Technical Physics, 50(10), 1311 (2005); https://doi.org/10.1134/1.2103277.
[14] V. I. Lysov, T. L. Tsaregradskaya, A. M. Kurylyuk, O. V. Turkov, G. V. Saenko,*Controlled nanostructuring from an amorphous state in multicomponental alloys based on cobalt*, Journal of physical studies, 22(3),3702 (2018);https://doi.org/10.30970/jps.22.3701.
[15] N. Bayr , V.S. Kolat, T. Izgi, S. Atalay, H. Gencer and P. Sovak,*Crystallisation Kinetics of Co75−xMxSi15B10 (M = Fe, Mn, Cr and x = 0, 5) Amorphous Alloys*, Acta physica polonica a;); https://doi.org/10.12693/APhysPolA.129.84
[16] M. G. Babych, M. I. Zakharenko, M. P. Semen'ko, Yu. A. Kunyts'ky, and D. S. Leonov,*Peculiarities of Cobalt Based Amorphous Alloys Crystallization*, Nanosystems, Nanomaterials, Nanotechnologies, 6 (1), 237 (2008);
[17] Bo Han Zhang, Jia Hao Liu, Hai Tao Zhou,*Comprehensive study of the crystallization behavior, thermal stability, and magnetic properties of Co66.5Si15.5B12Fe4Ni2 amorphous ribbon*,Journal of Non-Crystalline Solids,573 (1), 121132 (2021);https://doi.org/10.1016/j.jnoncrysol.2021.121132.

[18] Stepan Mudry, and Yulia Nykyruy,*Laser induced structure transformation in Co70Fe3Mn3.5Mo1.5B11Si11 amorphous alloy*, Materials Science-Poland, 32 (1), 28 (2014); https://doi.org/10.2478/s13536-013-0152-2.
[19] Yu Nykyruy, S. Mudry, I. Shtablavyi, A. Borisyuk, Ya Tsekhmister, I. Gnilitskyi,*Formation of laser-induced periodic surface structures on amorphous Fe- and Co-based alloys and its impact on magnetic properties*, Materials Chemistry and Physics, 287, (2022); https://doi.org/10.1016/j.matchemphys.2022.126317.
[20] V. I. Lysov, T. L. Tsaregradskaya, A. M. Kurylyuk, O. V. Turkov, G. V. Saenko,*Controlled nanostructuring from an amorphous state in multicomponental alloys based on cobalt*, Journal of Physical Studies 22(3), (2018); https://doi.org/10.30970/jps.22.3702.

Ю.С. Никируй[1], С.І. Мудрий[1], Ю.О. Кулик[1], В.В. Пруніца[1], А.К. Борисюк[2]

Магнітні властивості та нанокристалізація аморфного сплаву на основі кобальту

[1] *Львівський національний університет імені Івана Франка, Львів, Україна*
[2] *Національний університет «Львівська політехніка», Львів, Україна*

Магнітні властивості аморфного сплаву $Co_{57}Fe_5Ni_{10}Si_{11}B_{17}$ досліджували за допомогою вібраційного магнітометра та було визначено температуру Кюрі (560 К) і температуру початку кристалізації сплаву (760 К). Коерцитивна сила аморфного сплаву - 200 А/м, та намагніченість насичення - 65 $Ам^2/кг$. Аморфний сплав виготовлений у вигляді стрічки товщиною 30 мкм методом спінінгування з розплаву. Внутрішню структуру сплаву та нанокристалізаційну поведінку в мовах ізотермічних відпалів при температурах 723 - 1023 К при різних часах (до 120 хвилин) досліджували методом рентгенівської дифракції і рентгеноструктурного аналізу.

Ключові слова: аморфний сплав на основі кобальту, ДТА, термомагнітні криві, гістерезис, магнітні властивості, рентгенівська дифракція, нанокристалізація.